Available online at www.sciencedirect.com
SCIENCE DIRECT®
Biochemical and Biophysical Research Communications 330 (2005) 104–110
BBRC
www.elsevier.com/locate/ybbrc

# Loss of lysophospholipase 3 increases atherosclerosis in apolipoprotein E-deficient mice

Yoshio Taniyama [c,*,1], Hiromitsu Fuse [b,1], Tomoko Satomi [b], Ryuichi Tozawa [b], Yoshitaka Yasuhara [b], Kozo Shimakawa [b], Sachio Shibata [a], Masahiko Hattori [a], Mitsugu Nakata [b], Shigehisa Taketomi [b]

[a] *Pharmacology Research Laboratories II, Pharmaceutical Research Division, Takeda Pharmaceutical Company Limited, 10 Wadai, Tsukuba, Ibaraki 300-4293, Japan*
[b] *Pharmacology Research Laboratories I, Pharmaceutical Research Division, Takeda Pharmaceutical Company Limited, 17-85, Jusohonmachi 2-chome, Yodogawa-ku, Osaka 532-8686, Japan*
[c] *Biomedical Research Laboratories, Pharmaceutical Research Division, Takeda Pharmaceutical Company Limited, 17-85, Jusohonmachi 2-chome, Yodogawa-ku, Osaka 532-8686, Japan*

Received 11 February 2005

**Abstract**

Human LCAT-like lysophospholipase (LLPL), or lysophospholipase 3, was first identified in vitro, in foam cells derived from THP-1 cells. We demonstrated that LLPL was present in foam cells in the severe atherosclerotic lesions that develop in apolipoprotein E-null (*apoE*$^{-/-}$) mice. This indicated that LLPL might affect lipid metabolisms in foam cells and, therefore, atherogenesis. Accordingly, we created *LLPL*-knockout mice by gene targeting and crossed them with *apoE*$^{-/-}$ mice. We showed that the absence of LLPL increased lesion formation markedly in *apoE*$^{-/-}$ mice but had little effect on the plasma-lipid profile. In addition, *LLPL*-deficient peritoneal macrophages were more sensitive to apoptosis induced by exposure to oxidized low-density lipoprotein. LLPL might provide a link between apoptosis in macrophages and atherogenesis. Our data demonstrate that LLPL activity is anti-atherogenic and indicate that the regulation of this enzyme might be a novel drug target for the treatment of atherosclerosis.


*Keywords:* Acylceramide synthase; Atherosclerosis; Apoptosis; Knockout mice; LLPL; Oxidized LDL; Lysophospholipase 3; Lysosomal phospholipase A2; Macrophage

The *LLPL*/lysophospholipase 3 gene was originally discovered in a screen to identify genes involved in lipid metabolisms that were differentially expressed in THP-1-cells and the foam cells derived from them [1]. Although the amino-acid sequence of LLPL was 49% identical to that of human lecithin cholesterol acyltransferase (LCAT), it had no detectable LCAT activity. LLPL was found in human plasma and the purified recombinant protein hydrolysed lysophosphatidylcholine [1]. Recently, the enzyme was reported to be a transacylase that catalysed the formation of 1-*O*-acylceramide by transferring fatty acids from the *sn*-2 position of phosphatidylcholine or phosphatidylethanolamine to ceramide [2]. The enzyme has an optimal pH of 4.5, which indicates that it is an acidic PLA2 that might specifically function within lysosomes [2]. In addition, the enzyme was suggested to play a role in pulmonary surfactant catabolism [3].

Until now, there was no evidence for the relationship between atherogenesis and LLPL functions. In the

* Corresponding author. Fax: +81 6 6308 9021.
*E-mail address:* Taniyama_Yoshio@takeda.co.jp (Y. Taniyama).
[1] These authors contributed equally to this work.

0006-291X/$ - see front matter © 2005 Elsevier Inc. All rights reserved.
doi:10.1016/j.bbrc.2005.02.126

present paper, we address this matter by comparing the development of atherosclerotic lesions in mice lacking both *LLPL* and *apoE* with that in $apoE^{-/-}$ mice.

## Materials and methods

*Tissue preparation and immunohistochemistry.* Male 40-week-old $apoE^{-/-}$ mice fed on normal rodent chow (CE-2; Oriental Yeast) were anesthetized with diethyl ether and perfused intracardially with 4% paraformaldehyde in phosphate-buffered solution (PBS). The hearts and intact aortas were removed, fixed overnight at 4 °C, embedded in optimum cutting temperature (OCT) compound, and frozen. Sections (6 μm) were cut in a cryostat, from the bottom of the atria to the leaflet in the aortic sinus. Aortic valve sections were stained with haematoxylin–eosin and oil red O. Adjacent sections were immunostained with a rabbit polyclonal antibody against mouse FLAG-tagged LLPL, which was produced in insect cells. Alexa Fluor 488 goat anti-rabbit IgG (Molecular Probes) was used as a secondary antibody. Negative controls used antibody absorbed with excess mouse LLPL protein.

*Gene targeting.* The gene-targeting vector was constructed by subcloning an 11-kb *Eco*RI DNA fragment containing exons 1 and 2, and a 1.5-kb *Hin*dIII/*Pst*I DNA fragment containing part of exon 6 of the mouse *LLPL* gene into the *Not*I and *Xho*I sites, respectively, of the pPol II short-neob PA-HSVTK vector [4]. The vector was linearized by *Sal*I digestion and electroporated into embryonic stem (ES) cells from the 129/SvEv mouse strain (LEXICON). G418/1-(2-deoxy, 2-fluoro-β-D-arabinofuranosyl)-5-iodouracil (FIAU) resistant clones were screened using Southern blot analysis and ES cells carrying the disrupted allele were microinjected into C57BL/6 mouse blastocysts to produce chimaeric mice. These mice were intercrossed to produce homozygous $LLPL^{-/-}$ mice, which were then mated with $apoE^{-/-}$ mice on a C57BL/6 background (N10 C57Bl/6; Jackson Labs). $LLPL^{+/-}apoE^{+/-}$ mice were backcrossed to $apoE^{-/-}$ mice to produce $LLPL^{+/-}apoE^{-/-}$ mice, which were intercrossed to produce all three *LLPL* genotypes on the *apoE*-null background (87.5% C57BL/6: 12.5% 129/SvEv).

*Immunoblotting.* Peritoneal macrophages were elicited in $LLPL^{-/-}$ mice and their wild-type littermates by injecting 1.5 ml of 2% thioglycollate medium intraperitoneally. After 4 days, cell lysates were prepared using the Mammalian Protein Extraction Reagent (M-PER) (Pierce). Cell extracts (900 μl) plus 100 μl of 10× immunoprecipitation (IP)-buffer (20 mM Tris–HCl (pH 7.4), 150 mM NaCl, and 10% Triton X-100) were incubated overnight with either 10 μg of rabbit anti-mouse LLPL polyclonal antibody or non-immune rabbit IgG at 4 °C. Samples were then gently shaken overnight at 4 °C with 50 μl of anti-rabbit IgG–agarose (50% slurry; Sigma). The agarose beads were washed twice with IP-buffer, boiled for 5 min in 50 μl Laemmli sample buffer, centrifuged, and separated by non-reducing 12.5% SDS–PAGE. Gels were electro-transferred to PVDF membranes (Amersham Biosciences). The membranes were incubated with anti-human LLPL monoclonal antibody 1G, which cross-reacts with mouse LLPL, followed by HRP-conjugated anti-mouse IgG secondary antibody. Bands were detected using ECL Advance (Amersham) according to the manufacturer's instructions.

*Enzyme assay.* Tissues were homogenized in 10 mM Hepes (pH 7.4) and 0.25 M sucrose, and centrifuged at 100,000*g* for 60 min at 4 °C. 1-*O*-acylceramide synthase (ACS) activity was measured in the supernatants according to the method described by Abe et al. [5], using liposomes consisting of phosphatidylcholine (70 mol%), 1-palmitoyl-2-[$^{14}$C]arachidonyl-phosphatidylethanolamine (2 mol%), and dicetylphosphate (30 mol%). Liposomes (64 nmol phospholipid), 10 nmol C2-ceramide, and 5 μg bovine serum albumin (BSA) were added to the samples, which were made up to a volume of 500 μl with 50 mM sodium citrate (pH 4.5) and incubated for 30 min at 37 °C. The reaction was terminated by adding 3 ml chloroform/methanol (2/1) plus 0.3 ml of 0.9%(w/v) NaCl. After centrifugation for 5 min at 800*g*, the lower layers were transferred into fresh tubes and dried under nitrogen. The lipid extracts were separated on high-performance thin-layer chromatography (HPTLC) plates in chloroform/acetic acid (9:1). The radioactive spots were scraped off and analysed using liquid scintillation to quantify the products. The ACS activity was calculated as: specific dpm/mg protein/min/specific activity of [$^{14}$C]arachidonyl PE (dpm/pmol).

*Plasma lipid profile.* The plasma lipoprotein cholesterol was analysed using gel-permeation high-performance liquid chromatography (HPLC) and monitored by an on-line total cholesterol assay [6]. Plasma lipoproteins were separated on two connected columns (300 × 7.5 mm) of TSKgel Lipopropak XL (Tosoh) using TSK eluent LP-1 (Tosoh) buffer at a flow rate of 0.6 ml/min. Cholesterol was detected on-line by mixing the effluent from the columns with a commercial enzymatic reagent (Cholesterol E test Wako; Wako Pure Chemical Industries), which was continuously pumped at a flow rate of 0.3 ml/min. The enzymatic reaction at 45 °C in a reactor coil (7.5 m × 0.4 mm i.d.) was monitored for absorbance at 600 nm. A commercial standard for HDL-cholesterol serum measurement (Determiner Standard Serum; Kyowa Medex) was used to calibrate the system.

*Atherosclerotic-lesion analysis.* Mice were maintained on normal chow or on an atherogenic diet of normal chow supplemented with 7.5% cocoa butter, 1.25% cholesterol, 0.5% sodium cholate, 7.5% casein, 1.25% microcrystalline cellulose (Avicel), 1% vitamin mixture, 1% mineral mixture, 1.625% sucrose, 1.625% dextrose, 1.625% dextrin, and 0.125% choline chloride. Mice were sacrificed, and their hearts and aortas were perfused with saline through the left ventricle. The aortas were removed as close to the heart as possible and dissected from the aortic arch to just beyond the iliac bifurcation. They were then pinned onto black rubber boards, stained with oil red O, and fixed with 10% neutral buffered formalin. Images were captured with a Nikon COOLPIX990 digitalphoto camera, transferred to Adobe Photoshop, and both the total area of the aorta and the area of the atherosclerotic plaques were measured using Image Pro Plus Ver.4.5 (Media Cybernetics).

*Detection of apoptotic cells.* Thioglycollate-elicited peritoneal macrophages from $LLPL^{-/-}apoE^{-/-}$ mice and their $apoE^{-/-}$ littermates were incubated in Dulbecco's modified Eagle's medium (DMEM) supplemented with 10% heat-inactivated foetal bovine serum overnight. The medium was then changed to DMEM supplemented with 5 μg/ml copper-oxidized LDL [7] (oxLDL) with or without 5 μM DL-PPMP and was incubated for 24 h. Apoptotic cells were identified by staining with an Annexin-V-FLUOS Staining Kit (Roche Diagnostics GmbH) and were examined using fluorescence microscopy (Nikon Eclipse E600; Nikon).

## Results and discussion

### *The presence of LLPL in the atherosclerotic lesions in $apoE^{-/-}$ mice*

At first time, we examined whether LLPL is present in the atherosclerotic lesions in $apoE^{-/-}$ mice by immunohistochemistry and clearly demonstrated the presence of this enzyme in foam cells in atherosclerotic lesions in $apoE^{-/-}$ mice (Fig. 1). It suggested that LLPL might play a role in the development of atherosclerosis.

### *LLPL-knockout mice*

To better understand the biological function of LLPL, we used gene-targeting techniques to create *LLPL*-knockout mice. Mouse *LLPL* is 88% homologous

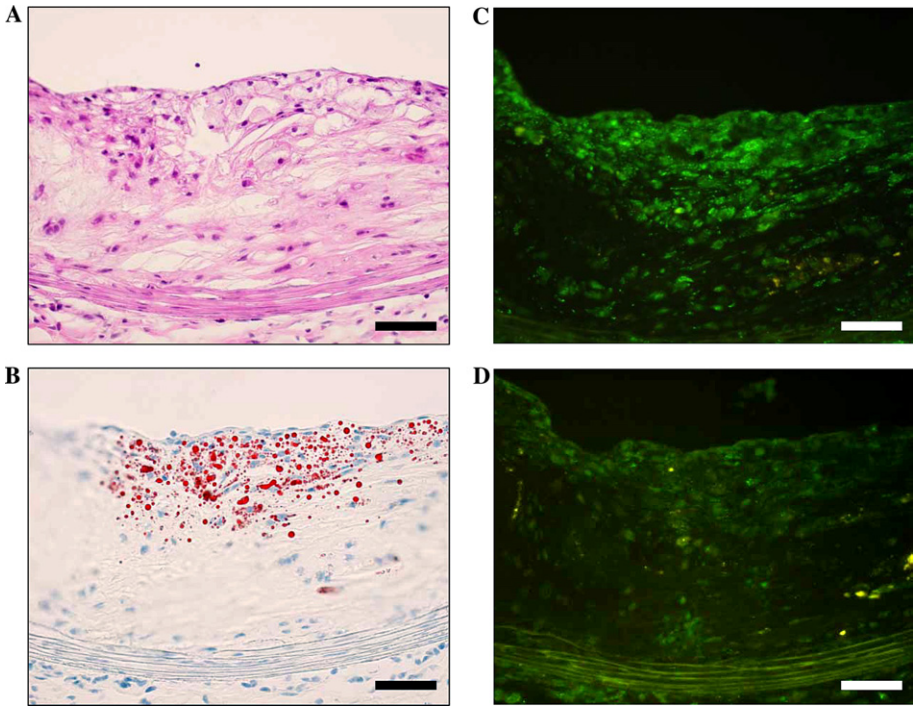


Fig. 1. Atherosclerotic lesions in apolipoprotein E-deficient mice. (A,B) Haematoxylin–eosin (A) and oil red O (B) staining of aortic valves. (C) The oil red O-positive area of the atherosclerotic lesion was also labelled using an anti-LLPL antibody. (D) Negative control for immunolabelling. Scale bar: 100 μm.

to the human gene [2] and contains a serine residue at the putative active site in exon 5. Therefore, *LLPL*-knockout ($LLPL^{-/-}$) mice were produced by targeted disruption of exons 3–5 (Fig. 2A). Homozygous mutant mice were identified using Southern blot analysis (Fig. 2B) and no LLPL protein was detected by immunoprecipitation in either the supernatant or cell lysates prepared from thioglycollate-elicited peritoneal macrophages (Fig. 2C).

The *LLPL*-mutant allele was transmitted in a Mendelian fashion, and *LLPL*-homozygous mutant mice were normal in their appearance and body weight when fed on a rodent chow diet (data not shown). Feeding both $LLPL^{-/-}$ and control mice an atherogenic diet led to increases in total cholesterol and LDL plus very-low-density lipoprotein (VLDL) cholesterol in the plasma (Figs. 3A and B). However, in $LLPL^{-/-}$ mice, the increases in cholesterol levels tended to be lower than those in control mice. These phenomena were particularly in male mice. Notably, none of the $LLPL^{-/-}$ mice, even when maintained on an atherogenic diet, showed evidence of atherosclerotic lesions (data not shown).

### *Advanced atherosclerotic lesions in $LLPL^{-/-}apoE^{-/-}$ mice*

To further investigate atherogenesis, $LLPL^{-/-}$ mice were intercrossed with $apoE^{-/-}$ mice to produce mice lacking both *LLPL* and *apoE* ($LLPL^{-/-}apoE^{-/-}$). Male mice were maintained on a normal diet and sacrificed at 18 weeks of age to determine the extent of aortic-lesion formation at a relatively early stage. Advanced atherosclerotic lesions were also examined in male mice that had been fed on a normal diet for 22 or 32 weeks. The lesions were measured en face in the whole aortic tree, and the percentages of the total surface area occupied by atherosclerotic lesions in the two groups are shown in Fig. 4A. The area of lesions in the aortic tree was larger in $LLPL^{-/-}apoE^{-/-}$ mice than in their $apoE^{-/-}$ littermates at all three time points. The area of atherosclerotic lesions was significantly increased in the aortas of $LLPL^{-/-}apoE^{-/-}$ mice compared to those of $apoE^{-/-}$ mice, in both the thoracic and abdominal regions (Fig. 4B). These results demonstrated that a deficiency of LLPL led to increased lesion formation in mice with an $apoE^{-/-}$ genetic background that were fed on a normal diet. However, when $LLPL^{-/-}apoE^{-/-}$ mice were fed on an atherogenic, Western-style diet [8], which produced exceptionally high plasma cholesterol levels (>1300 mg/dl), the extent of atherogenesis was no different from that in $apoE^{-/-}$ mice after 12–16 weeks (data not shown). These results show that if the plasma cholesterol level is exceedingly high, LLPL does not suppress lesion formation; however, at more moderate cholesterol levels, LLPL plays an anti-atherogenic role. Similar observations have been made for genes that are involved in immune responses, such as *CD40L* [9], *IFN-γ* [10], *RAG1*, and *RAG2* [11], which have also been reported to have atherogenic effects at moderate plasma cholesterol levels (600–800 mg/dl).

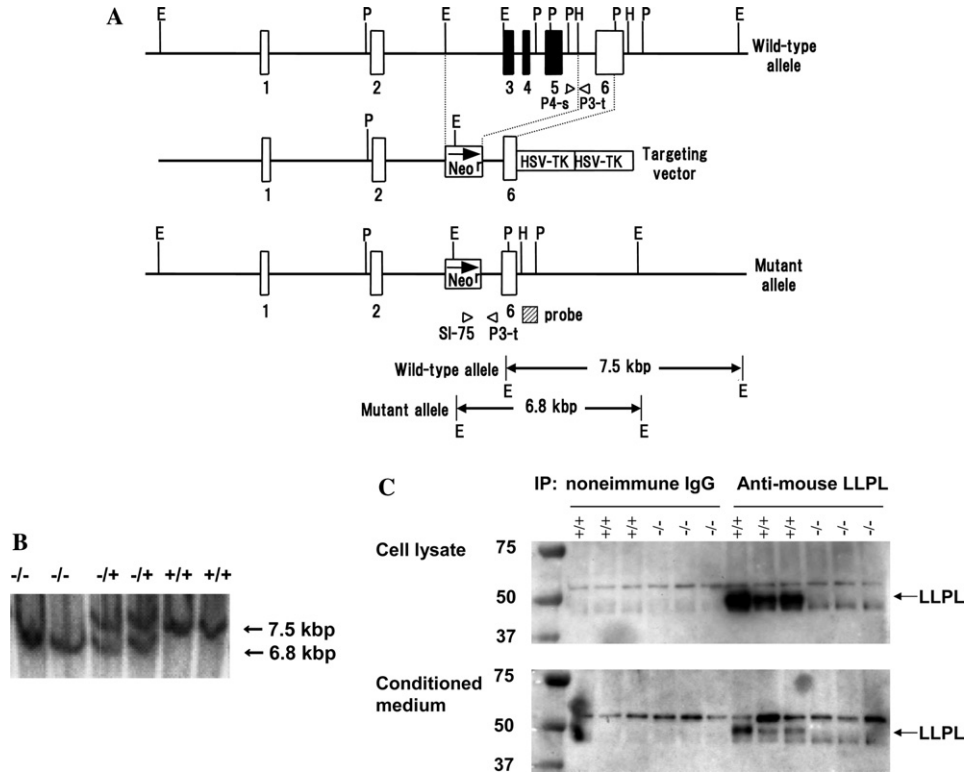


Fig. 2. Targeted disruption of the *LLPL* gene. (A) Restriction maps of the wild-type *LLPL* locus, targeting vector, and mutant allele. The *LLPL* locus was disrupted by replacing exons 3–5 (filled boxes) with the positive-selective marker Neo$^r$. Herpes simplex virus (HSV)-thymidine kinase (TK) was used for negative selection. The external probe used for genomic Southern blot analysis is shown in the crosshatched box. E, *Eco*RI; H, *Hin*dIII; and P, *Pst*I. (B) Southern blot analysis of mouse genomic DNA after *Eco*RI digestion and hybridization with the external probe. (C) Western blot analysis of intracellular and extracellular LLPL protein in cultured peritoneal macrophage. LLPL protein was immunoprecipitated from three wild-type (+/+) and *LLPL*$^{-/-}$ (−/−) mice with an anti-mouse LLPL polyclonal antibody or an irrelevant rabbit IgG. Arrows indicate the bands corresponding to LLPL protein.

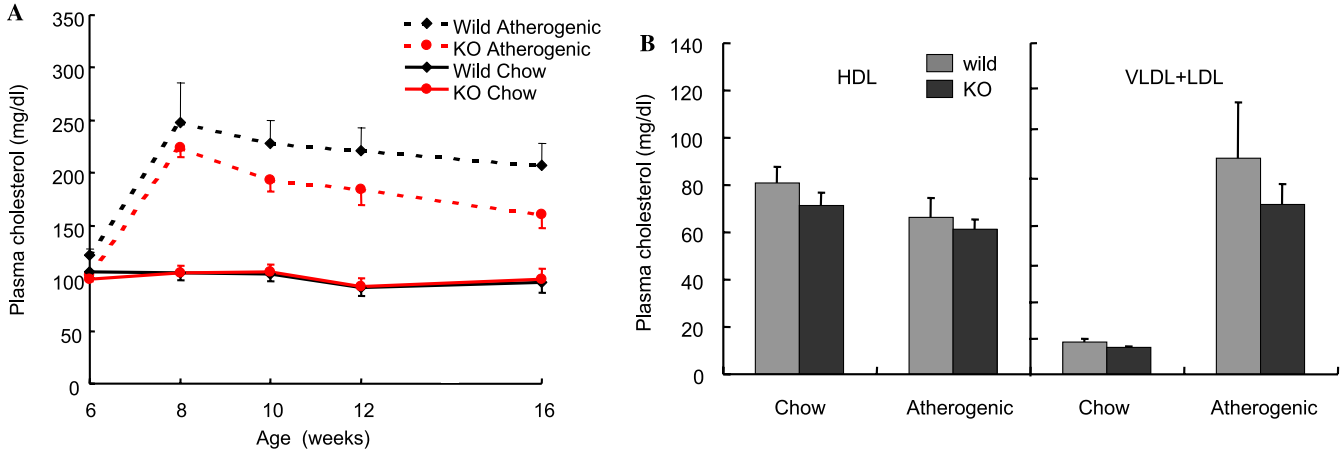


Fig. 3. Total cholesterol, HDL, and VLDL plus LDL cholesterol in plasma from *LLPL*$^{-/-}$ and control mice. Male 6-week-old *LLPL*$^{-/-}$ (KO) or wild-type (Wild) mice were fed on either chow or an atherogenic diet. (A) Time course of total plasma cholesterol. (B) Plasma HDL (left panel) and VLDL plus LDL (right panel) cholesterol in 16-week-old male mice. Data represent means ± SEM ($n = 5$–8).

*Plasma lipid profile*

To determine whether differences in lipid metabolism could account for the increased level of atherosclerosis in the *LLPL*$^{-/-}$*apoE*$^{-/-}$ mice, we measured total cholesterol and triglyceride levels in the plasma at 18, 22, and 32 weeks of age. Total cholesterol and triglyceride levels did not differ significantly between the LLPL genotypes at any time point and were within the range expected for *apoE*$^{-/-}$ mice maintained on a normal diet (Table 1). In addition, we analysed lipoprotein profiles at 18 weeks of age using gel-filtration chromatography, and found

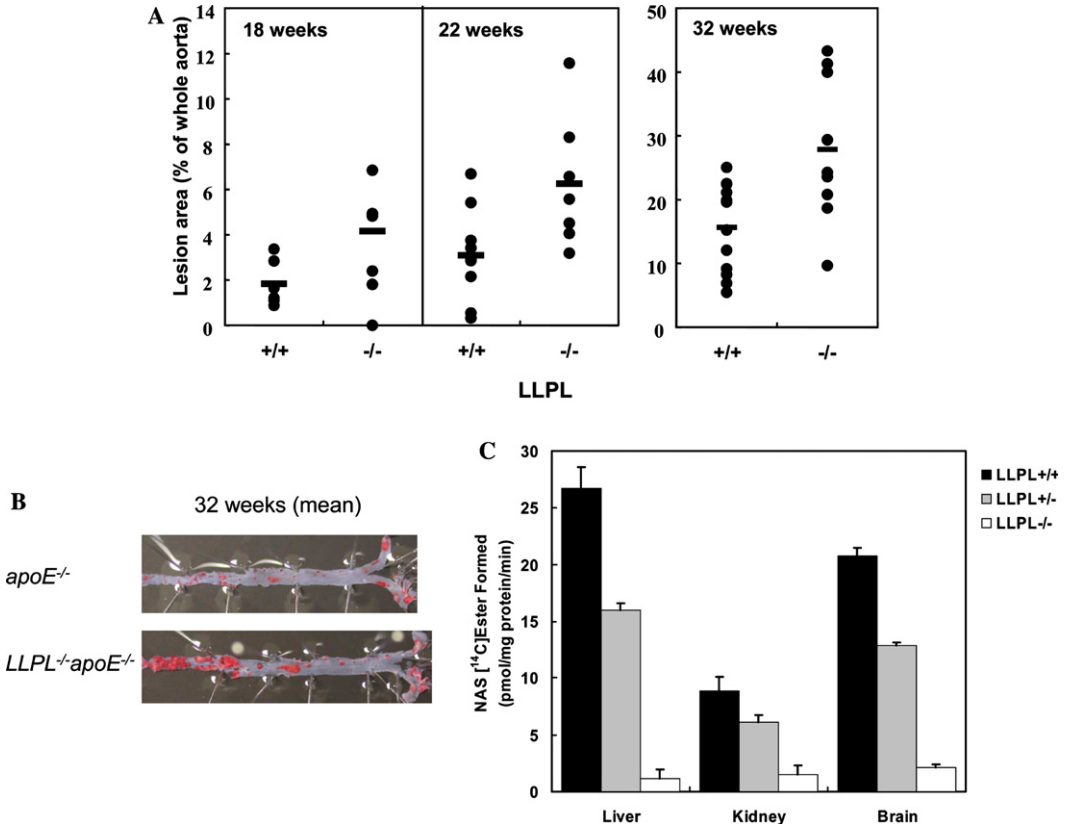


Fig. 4. Increased atherosclerotic lesion formation in $LLPL^{-/-}apoE^{-/-}$ mice and ACS activity in $LLPL^{-/-}apoE^{-/-}$, $LLPL^{+/-}apoE^{-/-}$, and $apoE^{-/-}$ mice. (A) $LLPL^{-/-}apoE^{-/-}$ and $apoE^{-/-}$ mice were fed on a normal chow diet for 18, 22, and 32 weeks. The lesion area was determined in en face aorta preparations. Each symbol represents one animal. Horizontal bars represent means. The differences between the genotypes are statistically significant (Dunnet-type test): $P < 0.05$ for $apoE^{-/-}$ mice ($n = 6$) versus $LLPL^{-/-}apoE^{-/-}$ ($n = 5$) at 18 weeks; $P < 0.05$ for $apoE^{-/-}$ mice ($n = 8$) versus $LLPL^{-/-}apoE^{-/-}$ ($n = 7$) at 22 weeks; and $P < 0.01$ for $apoE^{-/-}$ mice ($n = 10$) versus $LLPL^{-/-}apoE^{-/-}$ ($n = 9$) at 32 weeks. (B) Gross view of aortas stained with oil red O from $LLPL^{-/-}apoE^{-/-}$ (lower panel) and $apoE^{-/-}$ mice (upper panel) fed on a normal chow diet for 32 weeks. The red areas indicate the atherosclerotic lesion. (C) ACS activity in the liver, kidney, and brain were abolished in $LLPL^{-/-}$ mice (open bars). Data show means ± SEM.

Table 1
Body weight, total plasma cholesterol (TC), and plasma triglyceride (TG) levels in $LLPL^{-/-}apoE^{-/-}$ mice

| Age (weeks) | Genotype | $n$ | Body weight (g) | TC (mg/dl) | TG (mg/dl) |
|---|---|---|---|---|---|
| 18 | $apoE^{-/-}$ | 6 | 27.6 ± 1.0 | 909 ± 113 | 215 ± 43 |
| | $LLPL^{-/-}apoE^{-/-}$ | 5 | 25.7 ± 1.6 | 1195 ± 53 | 115 ± 21 |
| 22 | $apoE^{-/-}$ | 12 | 28.6 ± 0.5 | 1261 ± 46 | 191 ± 8 |
| | $LLPL^{-/-}apoE^{-/-}$ | 10 | 29.0 ± 1.4 | 1170 ± 44 | 183 ± 9 |
| 32 | $apoE^{-/-}$ | 12 | 30.0 ± 0.8 | 1200 ± 59 | 234 ± 33 |
| | $LLPL^{-/-}apoE^{-/-}$ | 9 | 30.9 ± 1.9 | 1034 ± 49 | 230 ± 20 |

Mice were maintained on a normal chow diet, and their body weight, TC, and TG levels were measured at 18, 22, and 32 weeks of age. All data are expressed as means ± SEM. No significant difference was noted between $LLPL^{-/-}apoE^{-/-}$ and $apoE^{-/-}$ mice.

similar plasma-lipoprotein profiles in $LLPL^{-/-}apoE^{-/-}$ mice and $apoE^{-/-}$ mice (data not shown). In $apoE^{-/-}$ mice, the size of the atherosclerotic lesions was influenced by high-density lipoprotein (HDL) levels [12]. However, the mean HDL cholesterol levels were similar in $apoE^{-/-}$ ($n = 6$) and $LLPL^{-/-}apoE^{-/-}$ ($n = 5$) mice (41 and 35 mg/dl, respectively), and appeared to be unaffected by the *LLPL* genotype. Furthermore, no differences were observed in the free HDL cholesterol level, which indicates that LLPL has no effect on LCAT activity (data not shown). These results strongly suggest that the increased lesion size in the $LLPL^{-/-}apoE^{-/-}$ mice was not explained by changes in plasma cholesterol levels or in the distribution of lipoprotein particles. We also measured the extent of oxidation in the plasma by monitoring the formation of thiobarbituric-acid-reacting substances (TBARS). No significant difference was detected in the concentration of TBARS in $apoE^{-/-}$ and $LLPL^{-/-}apoE^{-/-}$ mice at 18 weeks of age (54 ± 20 and 33 ± 7 nmol/ml, respectively), which indicates that LLPL has no effect on the oxidation status in the plasma.

*Transacylation activity of C2-ceramide in the mice homogenates*

Recently, it has been proposed that apoptotic cell death contributes to plaque instability, rupture, and thrombus formation [13]. Oxidized LDL (oxLDL) is present in atheromas and is the local source of lipid for cells in atherosclerotic lesions [14]. Ceramide levels and apoptosis have both been reported to be elevated in cells treated with oxLDL [15]. LLPL might transacylate ceramide under physiological conditions and, hence, play a primary role in apoptotic cell death by regulating intracellular levels of ceramide [2]. We therefore measured the transacylation activity [5] of C2-ceramide in liver, kidney, and brain homogenates from $LLPL^{-/-}$, $LLPL^{+/-}$, and $LLPL^{+/+}$ (wild-type) mice on an $apoE^{-/-}$ genetic background (Fig. 4C). Transacylase activity was absent in $LLPL^{-/-}$ mice and was approximately 50% of the wild-type level in $LLPL^{+/-}$ mice.

*Susceptibility of macrophage apoptosis induced by oxLDL*

To investigate the effects of LLPL deficiency on macrophage apoptosis, we compared the sensitivity of thioglycollate-elicited peritoneal macrophages from $LLPL^{-/-}$ $apoE^{-/-}$ and $apoE^{-/-}$ mice to apoptosis induced by oxLDL (5 μg/ml). This was performed in either the presence or absence of the reagent DL-threo-1-phenyl-2-palmitoylamino-3-morpholino-1-propanol (DL-PPMP; 5 μM) [16], which accelerates the intracellular accumulation of ceramide, by detecting annexin V binding to exposed phosphatidylserine as a marker of the early stages of apoptosis [17] (Fig. 5). Immunofluorescence microscopy showed that LLPL deficiency led to phosphatidylserine exposure under these conditions and this was accelerated by DL-PPMP (Fig. 5). This indicated that LLPL might function in preventing the apoptosis induced by oxLDL in two ways: first, the enzyme might transform excess ceramide into biologically inactive metabolites, such as 1-*O*-acylceramide, and so protect against apoptosis [2]; and second, the high sensitivity of *LLPL*-deficient mice to oxLDL might result from a lysosomal dysfunction, as oxLDL has been reported to be resistant to degradation and to accumulate in lysosomes [18]. As LLPL might be a lysosomal PLA2, it could be responsible for the catabolism of oxLDL phospholipids in macrophages in atherosclerosis.

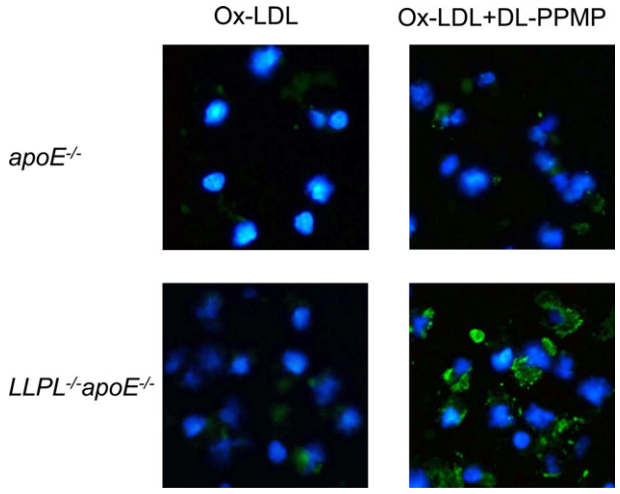


Fig. 5. Fluorescence microscopy showing phosphatidylserine externalization in peritoneal macrophages. Macrophages from $LLPL^{-/-}apoE^{-/-}$ and $apoE^{-/-}$ mice were treated with 5 μg/ml oxLDL in the absence or presence of 5 μM DL-PPMP. Cells were stained with 4′,6-diamidino-2-phenylindole (DAPI; blue) and fluorescein isothiocyanate (FITC)-labelled-annexin V (green), which indicate the presence of phosphatidylserine on extracellular-surface of the membrane. Original magnification: 20×.

In summary, our findings showed that, even in a severe model of atherosclerosis, LLPL exhibited a protective effect on atheroma formation at all stages and throughout the aortic tree in mice fed on normal diet. However, none of the $LLPL^{-/-}$ mice maintained on a chow or atherogenic diet showed evidence of atherosclerotic lesions, which indicates that hyperlipidaemia is a prerequisite for the development of such lesions. Although the physiological roles of LLPL remain to be determined, our results strongly suggest that LLPL has an important regulatory role in atherogenesis.

## Acknowledgments

We thank Drs. H. Sawada, T. Kurokawa, T. Wada, A. Nishimura, K. Yoshimura, H. Kasuga, and K. Kubo for useful discussions throughout this study, and also thank S. Nishizawa, K. Horikoshi, S. Kita, T. Asano, and T. Yano for assistance and discussions. We thank Dr. S. Ishibashi for useful advice on the construction of knockout mice. Finally, we thank the late Dr. M. Fujino for his encouragement of this study.

## References

[1] Y. Taniyama, S. Shibata, S. Kita, K. Horikoshi, H. Fuse, H. Shirafuji, Y. Sumino, M. Fujino, Cloning and expression of a novel lysophospholipase which structurally resembles lecithin cholesterol acyltransferase, Biochem. Biophys. Res. Commun. 257 (1999) 50–56.

[2] M. Hiraoka, A. Abe, J.A. Shayman, Cloning and characterization of a lysosomal phospholipase A2, 1-*O*-acylceramide synthase, J. Biol. Chem. 277 (2002) 10090–10099.

[3] A. Abe, M. Hiraoka, S. Wild, S.E. Wilcoxen, R. Paine III, J.A. Shayman, Lysosomal phospholipase A2 is selectively expressed in alveolar macrophages, J. Biol. Chem. 279 (2004) 42605–42611.

[4] S. Ishibashi, J.L. Goldstein, M.S. Brown, J. Herz, D.K. Burns, Massive xanthomatosis and atherosclerosis in cholesterol-fed low density lipoprotein receptor-negative mice, J. Clin. Invest. 93 (1994) 1885–1893.

[5] A. Abe, J.A. Shayman, N.S. Radin, A novel enzyme that catalyzes the esterification of N-acetylsphingosine, J. Biol. Chem. 271 (1996) 14383–14389.
[6] S. Usui, M. Nakamura, K. Jitsukata, M. Nara, S. Hosaki, M. Okazaki, Assessment of between-instrument variations in a HPLC method for serum lipoproteins and its traceability to reference methods for total cholesterol and HDL-cholesterol, Clin. Chem. 46 (2000) 63–72.
[7] T. Ohta, K. Takata, S. Horiuchi, Y. Morino, I. Matsuda, Protective effect of lipoprotein containing apolipoprotein A-I on $Cu^{2+}$-catalyzed oxidation of human low density lipoprotein, FEBS Lett. 257 (1989) 435–438.
[8] T. Yoshikawa, H. Shimano, Z. Chen, S. Ishibashi, N. Yamada, Effects of probucol on atherosclerosis of apoE-deficient or LDL receptor-deficient mice, Horm. Metab. Res. 33 (2001) 472–479.
[9] U. Schonbeck, P. Libby, CD40 signaling and plaque instability, Circ. Res. 89 (2001) 1092–1103.
[10] S. Gupta, A.M. Pablo, X. Jiang, N. Wang, A.R. Tall, C. Schindler, IFN-γ potentiates atherosclerosis in ApoE knock-out mice, J. Clin. Invest. 99 (1997) 2752–2761.
[11] H.M. Dansky, S.A. Charlton, M.M. Harper, J.D. Smith, B lymphocytes play a minor role in atherosclerotic plaque formation in the apolipoprotein E-deficient mouse, Proc. Natl. Acad. Sci. USA 94 (1997) 4642–4646.
[12] L. Boring, J. Gosling, M. Cleary, I.F. Charo, Decreased lesion formation in $CCR2^{-/-}$ mice reveals a role for chemokines in the initiation of atherosclerosis, Nature 394 (1998) 894–897.
[13] Z. Mallat, A. Tedgui, Current perspective on the role of apoptosis in atherothrombotic disease, Circ. Res. 88 (2001) 998–1003.
[14] S. Ehara, M. Ueda, T. Naruko, K. Haze, A. Itoh, M. Otsuka, R. Komatsu, T. Matsuo, H. Itabe, T. Takano, Y. Tsukamoto, M. Yoshiyama, K. Takeuchi, J. Yoshikawa, A.E. Becker, Elevated levels of oxidized low density lipoprotein show a positive relationship with the severity of acute coronary syndromes, Circulation 103 (2001) 1955–1960.
[15] S.M. Colles, J.M. Maxson, S.G. Carlson, G.M. Chisolm, Oxidized LDL-induced injury and apoptosis in atherosclerosis, Trends Cardiovasc. Med. 11 (2001) 131–138.
[16] Y. Lavie, H. Cao, A. Volner, A. Lucci, T. Han, V. Geffen, A.E. Giuliano, M.C. Cabot, Agents that reverse multidrug resistance, tamoxifen, verapamil, and cyclosporin A, block glycosphingolipid metabolism by inhibiting ceramide glycosylation in human cancer cells, J. Biol. Chem. 272 (1997) 1682–1687.
[17] G. Koopman, C.P. Reutelingsperger, G.A. Kuijten, R.M. Keehnen, S.T. Pals, M.H. van Oers, Annexin V for flow cytometric detection of phosphatidylserine expression on B cells undergoing apoptosis, Blood 84 (1994) 1415–1420.
[18] M. Lougheed, H.F. Zhang, U.P. Steinbrecher, Oxidized low density lipoprotein is resistant to cathepsins and accumulates within macrophages, J. Biol. Chem. 266 (1991) 14519–14525.